Insights into the Self-Assembly of Small, Organic Molecules: Case Study of 2,4,6-Trichlorophenol

Christophe Chipot

Laboratoire de Chimie Théorique, Unité Mixte de Recherche CNRS/UHP No. 7565 Institut Nancéien de Chimie Moléculaire, Université Henri Poincaré−Nancy I, B.P. 239, 54506 Vandœuvre-lès-Nancy, France

Received: February 14, 2001

Hybrid Monte Carlo and classical molecular dynamics simulations of a hydrated 2,4,6-trichlorophenol bilayer are presented. In line with recent freeze−fracture electron microscopy observations, the present investigation confirms that 2,4,6-trichlorophenol can form stable, lamellar structures. Self-assembly into a bilayer arises from strong dispersion forces that favor stacked arrangements of the monomers, as is demonstrated by high-level quantum chemical calculations. It also results from the subtle balance between hydrophobic and hydrophilic contributions, responsible for the preferential orientation of the aromatic compounds and the cohesion of the supramolecular arrangement. Imbalance of these contributions is illustrated in the case of 2,6-dichlorophenol that does not yield lamellar structures.

I. Introduction

To a large extent, predicting a priori the aptitude of a given molecule to form supramolecular structures remains a challenging task. In a number of obvious examples, self-assembly into complex, three-dimensional arrangements can be anticipated from the simple knowledge of the chemical nature of the surfactant.[1−5] In other, less intuitive instances, the criteria that determine the tendency of a molecule to self-organization into supramolecular structures are far more difficult to understand and delineate.[6] This is precisely the case of chlorophenols,[7] the saturated solutions of which show a natural propensity to yield a variety of three-dimensional assemblies, including long, transparent sheets and filaments.[8] Perhaps the most surprising result, explaining the observed unexpected morphologies, and unveiled by freeze−fracture electron microscopy, is the ability of such small, organic molecules to self-assemble into bilayers.[8] Considering the chemical features of chlorophenols, in sharp contrast with more traditional, amphipathic, often chiral surfactants, spontaneous aggregation leading to lamellar motifs[9−14] can only be rationalized by the subtle balance between hydophilic and hydrophobic contributions.[1,15] Whereas 2,4,6-trichlorophenol tends to self-assemble into bilayers, subsequently forming at the macroscopic level thin, transparent sheets writhing into helices before twisting ultimately into long filaments, optical transmission microscopy reveals that 2,6-dichlorophenol only yields rigid, brittle crystals.

The main thrust of this article is to provide the missing microscopic detail of the self-assembly of chlorophenols in water, inaccessible to experiment, using large-scale, statistical mechanics simulations, in conjunction with high-level quantum chemical calculations. If elucidating the underlying mechanisms accounting for the formation of meso- and macroscopic, three-dimensional structures clearly goes beyond the scope of the present contribution, our goal is to explain how small, organic molecules are capable of self-organizing into lamellar arrangements, thereby bridging theory to experiment. After summarizing in the following section the methodological details of the computations performed, the results of a simulation of a fully hydrated 2,4,6-trichlorophenol bilayer are discussed. Differences in the propensity to self-assemble into supramolecular structures is illustrated by comparing 2,6-dichlorophenol and 2,4,6-trichlorophenol.

II. Methods

The bilayer was constructed by replicating a single 2,4,6-trichlorophenol unit in the *x*- and *y*-directions of space, to form a leaflet of 55 molecules, and by generating a mirror image of the latter. The supramolecular assembly of 110 2,4,6-trichlorophenol molecules was subsequently placed between two lamellae of 1147 water molecules each. The fully hydrated bilayer was investigated in a so-called open geometry, whereby each water lamella is in equilibrium with its respective low-pressure vapor phase.

A hybrid Monte Carlo[16,17] (HMC) approach was employed to equilibrate the system in the (N, $P_\perp$, γ, T) thermodynamic ensemble. The normal pressure to the water liquid−vapor interface, $P_\perp$, the surface tension, γ, and the temperature, T, were set to 1 atm, the experimental value of 48.4 mN/m, and 297.1 K, respectively.[8] One HMC pass consisted of 250 molecular dynamics steps. The Newton equations of motion were integrated using a 1.5 fs time-step. Thorough equilibration proceeded over 17 500 HMC passes, until the molecular surface area per 2,4,6-trichlorophenol unit in the *x*- and *y*-directions reached a stable plateau, at ca. 36.8 Å^2.

The equilibrated system, of dimensions equal to ca. 45.0 × 45.0 Å^2 in the *x*- and *y*-directions, served as a starting point for a separate 2 ns MD simulation in the canonical ensemble, from which a statistical analysis of the structurally and thermodynamically relevant properties was performed. The equations of motion were integrated with a 1 fs time-step. The temperature was maintained at 297.1 K by rescaling velocities periodically.

All the simulations reported herein were carried out using a parallelized version of the MD program COSMOS.[18] Nonbonded interactions between water molecules and/or small, electrically neutral groups of 2,4,6-trichlorophenol were truncated smoothly beyond 9.0 Å by means of a polynomial

10.1021/jp0105793 CCC: $20.00
Published on Web 05/16/2001

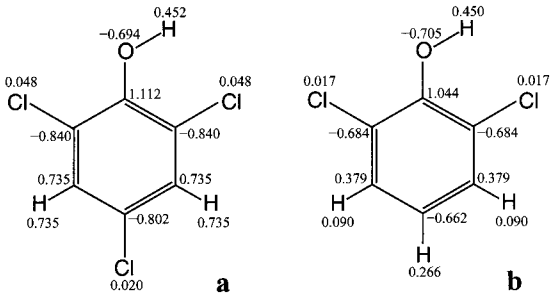

Figure 1. Point charge distribution of 2,4,6-trichlorophenol (a) and 2,6-dichlorophenol (b).

switching function applied over 0.5 Å.[19,20] The water molecules were described by the TIP4P potential energy function.[21] Intramolecular bond stretching, valence angle bending, torsion, out-of-plane, as well as van der Waals parameters for the HC, CA, OH, and HO atoms were taken from the AMBER all-atom force field.[22] Parameters characteristic of the chlorine atoms were adjusted to reproduce as accurately as possible the experimental free energy of hydration of 2,4,6-trichlorophenol, together with its quantum mechanically determined dimerization energy in the gas phase, yielding $R_{CL}^* = 1.95$ Å and $\epsilon_{CL} = 0.17$ kcal/mol. For the CA−CL stretching, the equilibrium bond length and force constant were 1.739 Å and 350 kcal/mol/Å, respectively. For the CA−CA−CL bending, the equilibrium valence angle and force constant were 120° and 70 kcal/mol/rad, respectively. Last, the parameters for the X−CA−CL−X torsion were $n = 2$, $V_n/2 = 0.27$ kcal/mol, and $\gamma = 180°$.

To compensate for induction effects, clearly absent in the pairwise additive potential energy function utilized, point charges were derived from the electrostatic potential[23,24] computed on a grid of points with a wave function perturbed by a continuum representation of the solvent.[25] A self-consistent reaction field[26] (SCRF) approach with an ellipsoidal cavity[27] surrounded by a dielectric medium of macroscopic permittivity equal to 78.3 were employed to obtain the electrostatic contribution to the solvent effect.[28] The fitted charges are given in Figure 1.

Using this effective model, the free energy of hydration of 2,4,6-trichlorophenol was estimated from a separate 20.8 ns simulation in the microcanonical ensemble, using the "umbrella sampling" approach.[29] In this calculation, the system consisted of a lamella formed by 490 TIP4P water molecules, in equilibrium, above and below it, with its vapor phase. The dimension of the cell in the *x*- and *y*-directions was 24.0 × 24.0 Å^2. The solute was translocated along the *z*-direction normal to the interface from far in the gas phase to the midst of the aqueous medium, using six mutually overlapping windows,[29,30] within which the solute was restrained by means of harmonic potentials. To enhance the sampling in each individual window, linear biases were added to the potential energy function. From the biased average probabilities of finding the solute in a given range along the *z*-direction, the complete free energy profile was constructed using the weighted histogram analysis method[31,32] (WHAM). The error associated with the free energy of hydration was estimated by breaking the overall simulation into three batches, from which a root-mean-squared deviation was derived.

III. Results and Discussion

A. Gas-Phase Dimerization Energies. The stacked arrangement of two 2,4,6-trichlorophenol molecules was investigated quantum mechanically at the MP2/6-31+G* level of approximation, using the GAUSSIAN 94 suite of programs.[33] This type of association is envisioned to yield the experimentally observed lamellar structures—2,4,6-trichlorophenol units piling up in the direction normal to the rings, and aggregating with neighboring stacks of aromatic molecules to form a two-dimensional leaflet. Although a true stacked motif, wherein the two rings are facing each other, is not favorable electrostatically, it, nevertheless, constitutes a reasonable model for investigating the dispersion contribution responsible for the binding of individual monomers. The geometry of a single 2,4,6-trichlorophenol molecule was first optimized using an MP2/6-311+G* wave function. The relative position of the two stacked monomers was determined by varying the distance separating the centroid of the rings by increments of 0.05 Å. At each step, the interaction energy was computed and corrected for the basis set superposition error (BSSE).[34] The optimal intermolecular distance was found at 3.9 Å, corresponding to a binding energy of −3.7 kcal/mol.

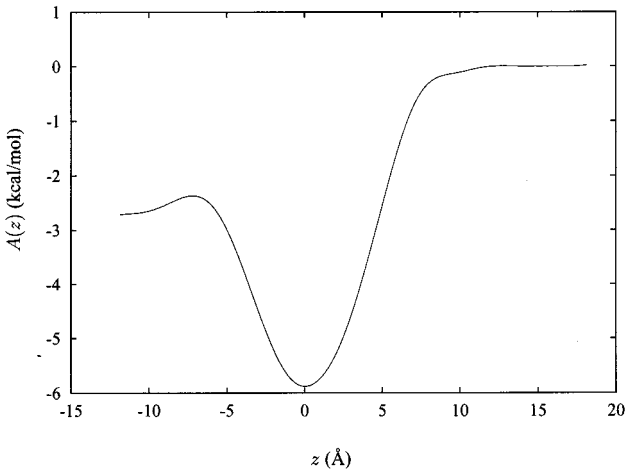

Figure 2. Free energy of 2,4,6-trichlorophenol at the water liquid−vapor interface. $z = 0$ corresponds to the Gibbs dividing surface. Positive and negative *z* values denote the gas and the aqueous phases, respectively. The hydration free energy of 2,4,6-trichlorophenol is the difference between the end points of the profile.

Employing the AMBER potential energy function[22] supplemented by van der Waals parameters optimized for chlorine atoms attached to aromatic rings, and point charges derived from the quantum chemical electrostatic potential,[23,24] the association energy of the stacked dimer was estimated at −4.6 kcal/mol. The distance separating the two monomers was found at 3.7 Å, slightly shorter than the ab initio value, which seems to indicate that the dispersion contribution in the molecular mechanics model is somewhat exaggerated.

B. Free Energy of Hydration. The free energy profile characterizing the transfer of one 2,4,6-trichlorophenol molecule from a low-pressure gaseous phase to the bulk of a water lamella is presented in Figure 2. For convenience, the average position of the water liquid−vapor interface has been shifted to $z = 0$ Å. From the onset, it can be seen that the curve exhibits a deep minimum near the Gibbs dividing surface, underlining the interfacial activity of the solute. This is not surprising considering the amphipathic character of 2,4,6-trichlorophenol, the hydroxyl group of which is buried in the aqueous medium while the nonpolar remainder of the molecule is exposed in large measure toward the vapor phase. The free energy of adsorption of the solute at the water liquid−vapor interface is −3.2 kcal/mol, close to the estimate of −2.8 kcal/mol for phenol by Pohorille and Benjamin.[35] The difference between the end points of the profile yields the free energy of hydration of 2,4,6-

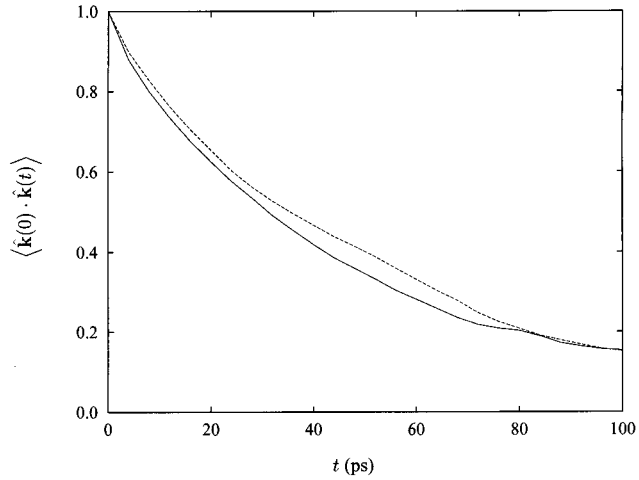

Figure 3. Time-correlation functions for the reorientation of 2,4,6-trichlorophenol about $\hat{\mathbf{u}}$, the vector borne by the C−O chemical bond (solid line) and $\hat{\mathbf{k}}$, the vector normal to the aromatic ring (dashed line).

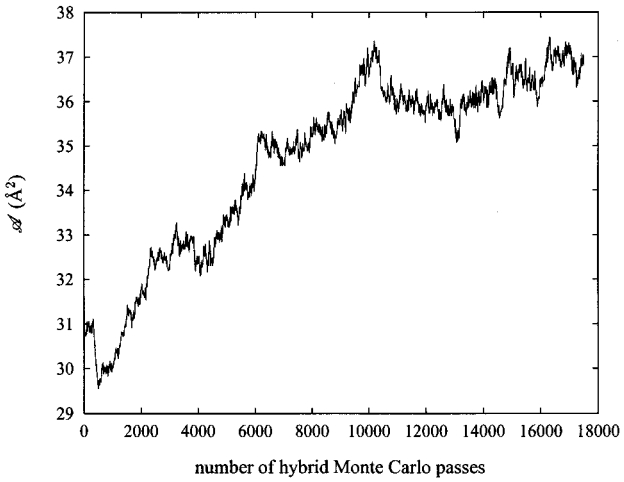

Figure 4. Evolution of the molecular surface area of 2,4,6-trichlorophenol in the bilayer during the equilibration process in the (N, $P_\perp$, γ, T) thermodynamic ensemble.

trichlorophenol, equal to -2.7 ± 0.3 kcal/mol. This result is somewhat underestimated in comparison with the value of -4.5 kcal/mol determined experimentally.[8] For the most part, the observed difference can be ascribed to an inadequate treatment of polarization effects.

This particular example illustrates the great difficulty in parametrizing pairwise additive potential energy functions capable of reproducing both gas-phase interaction energies and hydration free energies accurately. Usage of implicit polarization effects by means of distinct sets of point charges in the gas and the bulk phases could provide physically more realistic free energy estimates, albeit it is worth underlining that between the end points of the profile, the true charge distribution should be neither that for the vacuum nor that for the aqueous medium.

The length of this free energy simulation, 20.8 ns, might seem a priori excessive. It should be considered, however, that the reorientational times for 2,4,6-trichlorophenol are probably large, which explains that configurational space will be sampled slowly along the z reaction coordinate. To verify this hypothesis, a separate simulation of one 2,4,6-trichlorophenol molecule in a bath of 322 TIP4P water molecules was carried out at 298 K over 7.5 ns. From this additional run, the reorientational time correlation functions[20] with respect to the normal to the aromatic ring, $\hat{\mathbf{k}}$, and to the vector $\hat{\mathbf{u}}$ borne by the C−O chemical bond were computed. Integration of $\langle \hat{\mathbf{k}}(0)\cdot\hat{\mathbf{k}}(t)\rangle$ and $\langle \hat{\mathbf{u}}(0)\cdot\hat{\mathbf{u}}(t)\rangle$, shown in Figure 3, yields reorientational times equal to 52.1 and 49.2 ps, respectively. For comparison purposes, a similar simulation was performed, replacing the trichlorophenol molecule by a benzene one, for which the all-atom AMBER force field,[22] supplemented by potential derived point charges of -0.138 on the carbon atoms, was employed. Integration of the time correlation functions gives reorientational times of ca. 3 and 1 ps about the C_6 and the in-plane, C_2', axes, respectively, in line with the estimates of Linse.[36]

C. Water−Bilayer Arrangement. Figure 4 shows the evolution of the molecular surface area, A, of 2,4,6-trichlorophenol in the course of the HMC equilibration in the (N, $P_\perp$,γ, T) thermodynamic ensemble. Broadly speaking, over 10 000 passes were necessary to reach a plateau for A. This slow convergence is likely to be rooted in the HMC scheme itself, considering that the acceptance probability decreases with the square root of the number of particles constituting the system.[37] In the last 2000 HMC passes, the average molecular surface area was equal to ca. 36.8 Å^2, and the water−bilayer arrangement showed little fluctuations in its x,y-cross-section, with a root-mean-square deviation of ca. 0.3 Å^2.

The trajectory generated from the 2 ns simulation in the canonical ensemble was used for analyzing the structural properties of the hydrated 2,4,6-trichlorophenol bilayer. In Figure 5 a, the density profiles for the complete molecular system are reported. While a lamellar arrangement is characteristic here, the density profile for water extends sufficiently far within the phase formed by the aromatic compounds to suggest a significant flexibility of the complete assembly. In fact, in the middle of the bilayer, i.e., $z = 0$ Å, the probability for finding water molecules is nonzero, thereby indicating that the latter can migrate easily from the upper to the lower aqueous lamella, and vice versa. This result is not totally surprising considering the reduced thickness of the bilayer, and, more specifically, its hydrophobic region, as shown in the snapshot of Figure 5b.

On the basis of quantum chemical calculations of a stacked dimer of 2,4,6-trichlorophenol, it is anticipated that attractive $\pi-\pi$ interactions arising from dispersion forces could be responsible for the cohesion of the bilayer.[38,39] The probability distribution for angle ω formed by vectors $\hat{\mathbf{k}}$ and $\hat{\mathbf{k}}'$, the normals to a pair of distinct aromatic rings, reveals two very sharp maxima located at $\omega \simeq 14$ and 166° (see Figure 6). These peaks in $P(\omega)$ tend to indicate that the molecules of 2,4,6-trichlorophenol do not adopt a strict sandwich arrangement, but, more likely, a parallel-displaced one, whereby two neighboring rings are only partially stacked to minimize repulsive, electrostatic interactions—as has been observed, for instance, in the case of benzene.[40]

At the same time, as shown in Figure 7, the probability distribution for angle θ formed by vector $\hat{\mathbf{k}}$ and $\hat{\mathbf{n}}$, the normal to the water-bilayer interface, corrected for the Jacobian, exhibits a sharp peak at $\theta = 90°$. This maximum of $P_{\mathrm{corr}}(\theta)$demonstrates that, throughout the canonical simulation, the 2,4,6-trichlorophenol rings remain perpendicular on average to the aqueous interface. The slight asymmetry witnessed in the wings of the profile is likely to result from statistical inaccuracies. Interestingly enough, it can be noted that $P_{\mathrm{corr}}(\theta)$ follows a normal distribution and can, thus, be modeled by a Gaussian function with its maximum located at $\theta = 89.8°$ and the width at mid-height, $\sigma = 13.4°$.

The free energy for aligning the dipole, $\boldsymbol{\mu}$, or $\hat{\mathbf{u}}$, the vector borne by the C−O chemical bond, of the 2,4,6-trichlorophenol

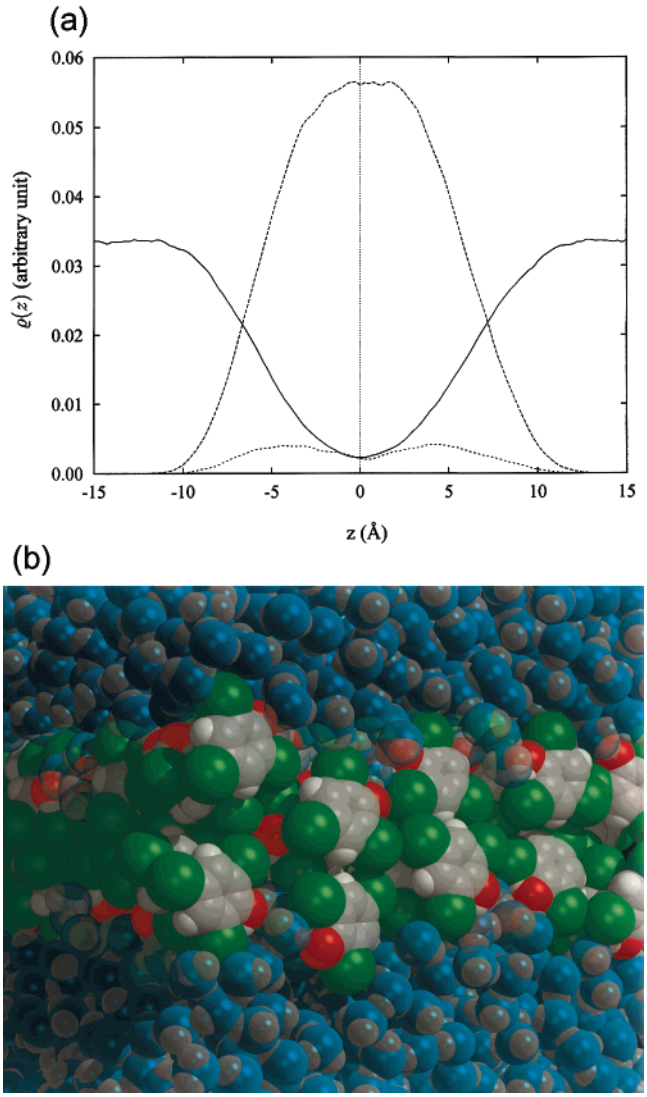

Figure 5. (a) Density profiles of the hydrated 2,4,6-trichlorophenol bilayer: Water (solid line), 2,4,6-trichlorophenol (long dashed line) and hydroxyl oxygen atoms (short dashed line). $z = 0$ denotes the center of the bilayer. (b) Cross-sectional view of the simulation cell in the *x*- and *y*-directions. The brighter, *y*, side of the box (right) highlights the bilayer arrangement of the 2,4,6-trichlorophenol units, with their hydroxyl moieties pointing toward the aqueous medium. The darker, *x*, side (left) clearly shows the stacking of the aromatic rings. Color code for 2,4,6-trichlorophenol: hydrogen, white; carbon, gray; oxygen, red; chlorine, green. For the semi-transparent water molecules: hydrogen, white; oxygen: blue.

molecules along $\hat{\mathbf{n}}$, the normal to the interface is reported in Figure 8 as a function of angle $\varphi \equiv (\hat{\boldsymbol{\mu}}, \hat{\mathbf{n}})$. Two orientations of the aromatic rings are clearly preferred, corresponding roughly to $\varphi = 50$ and 120°, with a free energy barrier separating the two minima of less than $2k_BT$. The first value characterizes those molecules forming the upper leaflet of the bilayer, whereas the second refers to those of the lower leaflet. It is obvious from this free energy profile that orientations for which, or $\hat{\mathbf{u}}$, and $\hat{\mathbf{n}}$ are either parallel or antiparallel are disfavored. Indeed, $\varphi = 0$ and 180° correspond to the largest sterical hindrances arising from the contact of chlorine atoms pertaining to the rings of the upper and the lower leaflets.

The concept of radial distribution function[41] (RDF) is not physically meaningful for anisotropic systems, because the density of sites *j*, ρ_j, in $g_{ij}(r) = \langle N_j(r; r + \delta r)\rangle / 4\pi\rho_j \int_r^{r+\delta r} dr\, r^2$ (where $\langle N_j(r; r + \delta r)\rangle$ is the average number of sites *j* located in the spherical layer of thickness δr centered about *i*) is

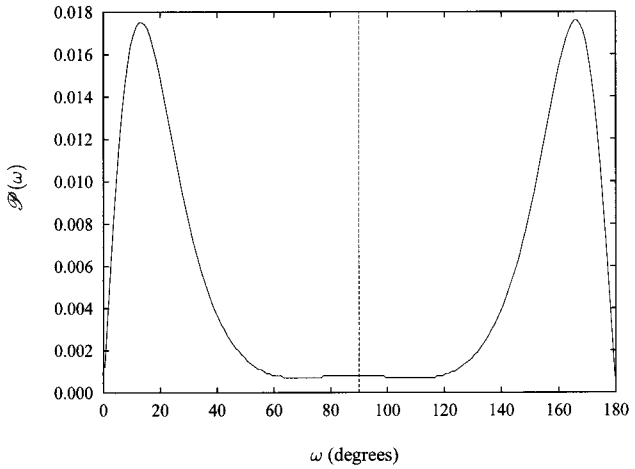

Figure 6. Probability distribution of angle, ω, formed by two vectors, $\hat{\mathbf{k}}$ and $\hat{\mathbf{k}}'$, normal to the aromatic ring in the 2,4,6-trichlorophenol bilayer.

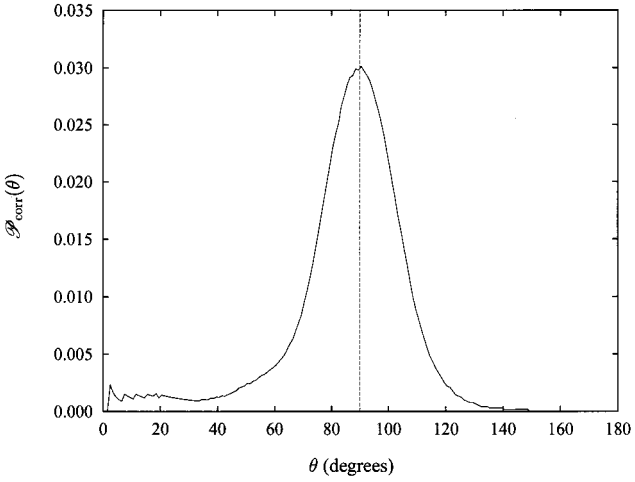

Figure 7. Corrected probability distribution of angle, θ, formed by $\hat{\mathbf{k}}$, the normal to the aromatic ring, and $\hat{\mathbf{n}}$, the normal to the water/2,4,6-trichlorophenol bilayer interface.

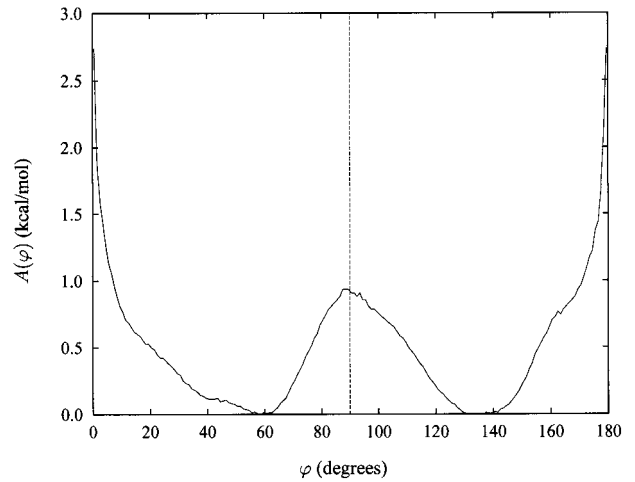

Figure 8. Free energy for aligning the dipole of 2,4,6-trichlorophenol and $\hat{\mathbf{n}}$, the normal to the water/bilayer interface.

inherently a function of *z*, the direction normal to the water-bilayer interface. As a result, the water oxygen atom−hydroxyl oxygen atom RDF, $g_{OO(water)}(r)$, is unlikely to converge toward 1.0 when the interatomic distance, *r*, increases. To estimate the coordination number of sites *i*, it seems, therefore, more appropriate to evaluate $\langle N_j(r; r + \delta r)\rangle$ as a function of *r*, either for the upper or for the lower leaflet/water lamella, and

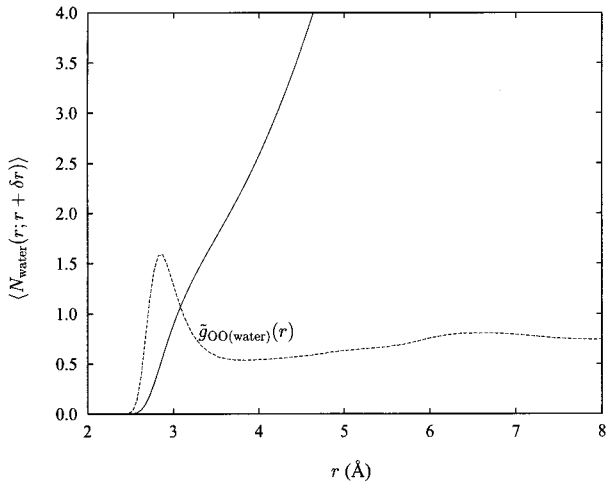

Figure 9. Average number of water molecules around the hydroxyl group of 2,4,6-trichlorophenol, $\langle N_{water}(r; r + \delta r)\rangle$ (solid line), and corresponding approximate radial distribution function, $\tilde{g}_{OO(water)}(r)$ (dashed line). The value of $\langle N_{water}(r; r + \delta r)\rangle$ at the first minimum of $\tilde{g}_{OO(water)}(r)$ gives the number of water molecules attached around each hydroxyl oxygen atom in the first shell of hydration.

determine its value at the first minimum of a qualitative RDF, $\tilde{g}_{ij}(r)$, computed using the above expression. The coordination number of the oxygen atom of 2,4,6-trichlorophenol in a bilayer arrangement can be derived from $\langle N_{water}(r; r + \delta r)\rangle$, presented in Figure 9. At $r = 3.8$ Å, corresponding to the limit of the first shell of hydration in $\tilde{g}_{OO(water)}(r)$, $\langle N_{water}(r; r + \delta r)\rangle \simeq 2$, indicating that each oxygen atom is, broadly speaking, bonded to two water molecules.

The average orientation of water molecules around the hydroxyl group of 2,4,6-trichlorophenol molecules in the bilayer can be determined by examining the distribution of the angle formed by the dipole moment of water and the vector pointing from the oxygen atom of water to that of 2,4,6-trichlorophenol—graph not shown here. A peak located around $r = 2.6$ Å indicates that hydrogen atoms of the surrounding water molecules point preferentially toward the oxygen atom of the hydroxyl groups. Beyond 4 Å, however, there is no clear-cut orientational preference of the water molecules. The slight, yet continuous decrease of the distribution observed after 8 Å is likely to be an artifact of the spherical truncation used for this study.

D. 2,4,6-Trichlorophenol versus 2,6-Dichlorophenol. Experimental observations reveal that, depending on the number of chlorine atoms and their relative position on the aromatic ring, hydrated chlorophenols can form or not supramolecular structures such as bilayers. Whereas 2,4,6-trichlorophenol shows a striking propensity to yield lamellar arrangements, as has been confirmed here by means of statistical simulations and experimentally, using freeze−fracture electron microscopy, 2,6-dichlorophenol does not share this unique property.[8] Why is it so? A plausible answer lies in the absence of chlorine atoms in the region separating the two chlorophenol leaflets, and the resulting loss of dispersion forces to warrant the cohesion of the bilayer.

This lack of dispersion forces is clearly visible in the association of two 2,6-dichlorophenol monomers. Molecular mechanical geometry optimization of the stacked dimer gives an interaction energy of −3.2 kcal/mol, i.e., 1.4 kcal/mol higher than that of its 2,4,6-trichlorophenol homologue, and a virtually unchanged intermolecular distance, viz., 3.7 Å.

Free energy perturbation[42] (FEP) calculations, wherein the chlorine atom in the para position is replaced by a hydrogen atom, were carried out for two distinct cases. In the first, a single, hydrated 2,4,6-trichlorophenol unit was mutated into 2,6-dichlorophenol to estimate the relative affinity of these two molecules for water. In the second, the 110 aromatic molecules that form the lamellar arrangement were mutated concurrently to yield a hydrated 2,6-dichlorophenol bilayer. In each case, the initial, i.e., 2,4,6-trichlorophenol, and the final, i.e., 2,6-dichlorophenol, states were divided into three successive steps. First, the point charge distribution of 2,4,6-trichlorophenol was mutated into that of 2,6-trichlorophenol —viz., ΔA_{elec}. Next, the CA−CL bond was shrunk to that characteristic of CA−HA—*viz.*, ΔA_{bond}. This value corresponds to the difference between the quantities estimated in the aqueous medium and in the gas phase.[43−45] Last, the van der Waals parameters of the para CL atom were replaced by those of HA—*viz.*, ΔA_{vdW}.

Starting from the simulation of 2,4,6-trichlorophenol in a bath of 322 TIP4P[21] water molecules used to estimate reorientational correlation times, the solute was mutated into 2,6-dichlorophenol. Each step of the mutation consisted of three windows involving 50 ps of equilibration followed by 100 ps of data collection. The error on the computed free energy was estimated by performing the same simulation three times with a different set of initial positions and velocities. The three contributions were found to be $\Delta A_{elec} = -1.1 \pm 0.0$ kcal/mol, $\Delta A_{bond} = +0.4 \pm 0.2$ kcal/mol and $\Delta A_{vdW} = -1.2 \pm 0.1$ kcal/mol, giving a net free energy change equal to -1.9 ± 0.2 kcal/mol, not too surprising considering the more polar character of 2,6-dichlorophenol (see Figure 1).

Concurrent mutation of the 110 2,4,6-trichlorophenol units forming the bilayer proceeded, starting from the last configuration of the (N, $P_\perp$, γ, T) equilibration. Considering the size of the system, an accurate determination of the total alchemical free energy change for sustituting all CL atoms in the para position by HA ones seems illusory, as it would require a considerable computational effort to reach appropriate convergence. Rather than providing such a free energy difference, the estimate of which clearly goes beyond the scope of this contribution, the emphasis was put on the cohesion of the mutated bilayer. The transformation was carried out using the protocol described above. It is worth underlining that the simulation performed in the canonical ensemble prevents the size of the cell from adjusting as the van der Waals radius of the para CL atom is decreased. Yet, in the x,y-plane, the molecular surface area of 2,6-dichlorophenol is anticipated to be close enough to that of 2,4,6-trichlorophenol. Furthermore, the open geometry, whereby the two water lamellae are in equilibrium with their respective vapor phases, should allow the thickness of the bilayer to adjust as mutation of the van der Waals radii and shrinking of the corresponding chemical bonds proceed.

The mutated bilayer was subsequently equilibrated over 0.5 ns, prior to an additional 1.5 ns production simulation in the canonical ensemble, aimed at probing the cohesion of the lamellar structure with time. Whereas the 2,4,6-trichlorophenol bilayer was characterized by a strong anisotropy in the orientation of the aromatic rings, as demonstrated by the probability distribution, $P(\omega)$, in Figure 6, its 2,6-dichlorophenol homologue does not show the same tendency. In fact, the order of the self-assembled structure rapidly vanishes, the orientation of the 2,6-dichlorophenol rings becoming increasingly isotropic. As can be seen in Figure 10, the two peaks of $P(\omega)$, reflecting the stacked arrangement of the 2,4,6-trichlorophenol units, coalesced into a quasi-continuuous distribution over all values of $\omega \equiv (\hat{\mathbf{k}}, \hat{\mathbf{k}}')$ angles. It should be noted, however, that the maximum of $P(\omega)$ emerges at ca. 90°, which reveals a marked

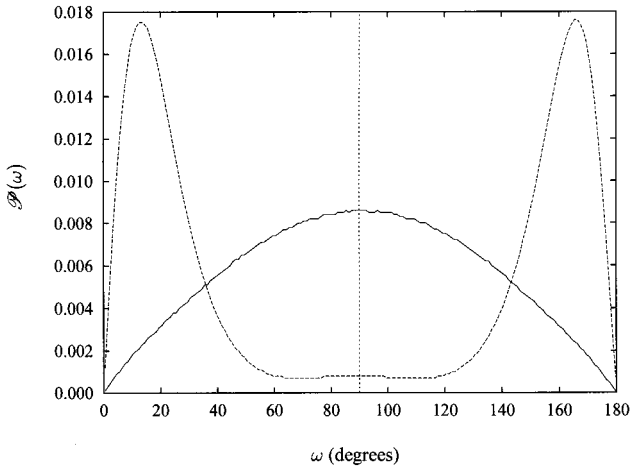

Figure 10. Probability distribution of angle, ω, formed by two vectors, $\hat{\mathbf{k}}$ and $\hat{\mathbf{k}}'$, normal to the aromatic ring in the 2,6-dichlorophenol bilayer (solid line). Comparison with the distribution characterizing the 2,4,6-trichlorophenol bilayer (dotted line).

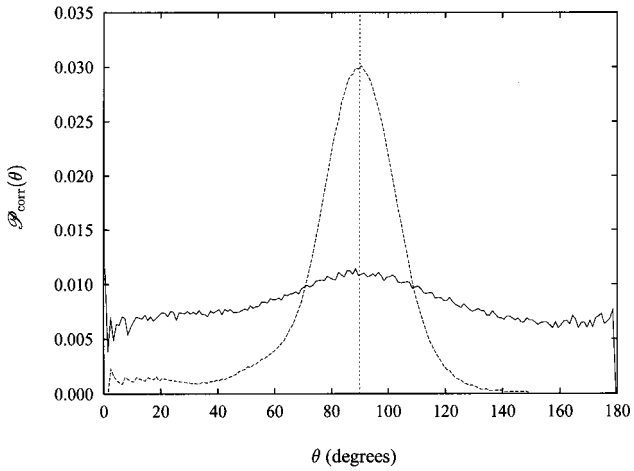

Figure 11. Corrected probability distribution of angle, θ, formed by $\hat{\mathbf{k}}$, the normal to the aromatic ring, and $\hat{\mathbf{n}}$, the normal to the water/2,6-dichlorophenol bilayer interface (solid line). Comparison with the distribution characterizing the 2,4,6-trichlorophenol bilayer (dotted line).

tendency to form T-shaped motifs, as has been reported, for instance, in the case benzene.[38,39] Moreover, the propensity of the aromatic compounds to remain perpendicular to the water-bilayer interface disappears, as demonstrated by the noteworthy widening of the $P_{\mathrm{corr}}(\theta)$distribution in Figure 11. This distribution cannot be modeled by a Gaussian function. The profile is reasonably flat, suggesting that all values of θ are sampled. Its maximum, still located around $\theta = 90°$, is significantly wider than for 2,4,6-trichlorophenol, and is only marginal. Put together, these data clearly suggest that a lamellar arrangement no longer exists, and that reversible aggregation to return to a bilayer is unlikely to occur.

In all likelihood, the witnessed differences in the behavior of the two seemingly similar aromatic species can be rationalized by the balance of hydrophobic and hydrophilic forces.[1,3,15] In the case of 2,4,6-trichlorophenol, the molecular mechanical association energy and the free energy of hydration are equal to -4.6 and -2.7 ± 0.3 kcal/mol, respectively. For 2,6-dichlorophenol, these quantities amount to -3.2 and -4.6 ± 0.5 kcal/mol, respectively. Propensity for aggregation into stacked motifs, thus, decreases, while affinity for water increases. Clearly, the replacement of a chlorine atom in the para position by a hydrogen atom entails an imbalance responsible for a preferential association of 2,6-dichlorophenol rings with surrounding water molecules. This behavior is consistent with the experimental observation that hydrated 2,6-dichlorophenol molecules do not self-assemble into lamellar structures.[8]

IV. Conclusion

To shed light on the mechanism of self-assembly of small, organic molecules, HMC[16,17] and classical MD simulations were carried out on a fully hydrated bilayer of 2,4,6-trichlorophenol. These simulations reveal that the system remains perfectly lamellar over the time-scale explored, in line with freeze−fracture electron microscopy experiments.[8] In contact with the aqueous environment, the amphipathic character of 2,4,6-trichlorophenol manifests itself by orienting the aromatic rings in a way that preserves hydration of the hydroxyl group while nonpolar moieties of the molecule interact favorably with equally nonpolar regions of neighboring aromatic species. High-level quantum chemical calculations suggest that aggregation of 2,4,6-trichlorophenol units is an organized process, whereby aromatic rings pile up in a stacked arrangement, driven by significant, attractive $\pi-\pi$ interactions.[38−40] Formation of the leaflet in the interfacial, *x*, *y*-plane in envisioned to result from additional, favorable dispersion interactions of the stacked rings. In-depth analysis of the MD trajectory confirms, indeed, that throughout the simulation, the participating aromatic rings are preponderantly stacked, or parallel-displaced, remaining oriented perpendicularly to the water−bilayer interface.

Comparison of 2,4,6-trichlorophenol and 2,6-dichlorophenol indicates that the presence of a chlorine atom in the para position is pivotal for the formation and intrinsic stability of the bilayer. The present series of statistical simulations reveal that whereas the former chlorophenol yields a lamellar arrangement, the latter does not.

The formation of complex morphologies, e.g., ribbons twisting into filaments, witnessed by transmission optical microscopy, remains a puzzling issue that the present set of simulations is unlikely to address. The structural features of these aggregates can only be attained at the meso- or macroscopic level, while simulations only provide the microscopic detail of experimentally observed phenomena. While experiment appears to rule out the necessity of a molecule to be chiral to obtain coiled macroscopic structures, the simulations reported herein support the view that coiling motions could result from the anisotropy in the self-assembly of chlorophenols in the *x*- and *y*-directions that form the plane of the interface. It could also be ascribed to the tilting of the stacked monomers, that associate preferentially in a parallel-displaced fashion.[40] Such assumptions should only find their validation when significantly larger patches of the hydrated bilayer are simulated.

Acknowledgment. The CENTRE CHARLES HERMITE, Vandœuvre-lès-Nancy, France, is gratefully acknowledged for generous allocation of computer time. The author is indebted to Dr. Michael H. New for helpful comments on HMC, to Dr. Raphaël Couturier for his involvement in the development of a parallel version of COSMOS, and to Dr. Ewa Rogalska for inspiring the topic of this article, and for fruitful and stimulating discussions. The Institut Nancéien de Chimie Moléculaire (INCM) is acknowledged for supporting this project.

References and Notes

(1) Tanford, C. *Science* **1978**, *200*, 1012.

(2) Gennis, R. B. *Biomembranes: Molecular Structure and Function*; Springer: New York, 1989.

(3) Israelachvili, J. *Intermolecular and surface forces*; Academic Press: London, 1992.

(4) Lasic, D. D. *Liposomes: From physics to applications*; Elsevier: Amsterdam, 1993.
(5) Deamer, D. W.; Fleischaker, G. R. *Origins of life: The central concepts*; Jones and Bartlett: Boston, 1994.
(6) Yager, P.; Chappell, J.; Archibald, D. D. When lipid bilayers will not form liposomes, tubules, helices and cochleate cylinders. In *Biomembrane structure and function: The state of the art*; Geber, B. P., Easwaran, K. R. K., Eds.; Adenine; Guilderland, NY, 1992; pp 1−19.
(7) Shiu, W. Y.; Ma, K. C.; Varhanickova, D.; Mackay, D. *Chemosphere* **1994**, *29*, 1155.
(8) Rogalska, E.; Rogalski, M.; Gulik-Krzywicki, T.; Gulik, A.; Chipot, C. *Proc. Natl. Acad. Sci. U.S.A.* **1999**, *96*, 6577.
(9) Schoen, P. E.; Price, R. R.; Schnur, J. M.; Gulik, A.; Gulik-Krzywicki, T. *Chem. Phys. Lipids* **1993**, *65*, 179.
(10) Schnur, J. M. *Science* **1993**, *262*, 1669.
(11) Thomas, B. N.; Safinya, C. R.; Plano, R. J.; Clarke, N. A. *Science* **1995**, *267*, 1635.
(12) Lipowsky, R. *Curr. Opin. Struct. Biol.* **1995**, *8*, 531.
(13) Terech, P.; Weiss, R. G. *Chem. Rev.* **1997**, *97*, 3133.
(14) Cornelissen, J. J. L.; Fischer, M.; Sommerdijk, N. A. J. M.; Nolte, R. R. M. *Science* **1998**, *280*, 1427.
(15) Paulaitis, M. E.; Garde, S.; Ashbaugh, H. S. *Curr. Opin. Coll. Interface Sci.* **1996**, *1*, 376.
(16) Duane, S.; Kennedy, A. D.; Pendleton, B. J.; Roweth, D. *Phys. Lett. B* **1987**, *195*, 216.
(17) Mehlig, B.; Herrmann, D. W.; Forrest, B. M. *Phys. Rev. B* **1992**, *45*, 679.
(18) Owenson, B.; Wilson, M. A.; Pohorille, A. *COSMOS*—A software package for COmputer Simulations of MOlecular Systems; NASA, Ames Research Center, Moffett Field, CA 94035-1000, 1987.
(19) Andrea, T. A.; Swope, W. C.; Andersen, H. C. *J. Chem. Phys.* **1983**, *79*, 4576.
(20) Allen, M. P.; Tildesley, D. J. *Computer Simulation of Liquids*; Clarendon Press: Oxford, 1987.
(21) Jorgensen, W. L.; Chandrasekhar, J.; Madura, J. D.; Impey, R. W.; Klein, M. L. *J. Chem. Phys.* **1983**, *79*, 926.
(22) Cornell, W. D.; Cieplak, P.; Bayly, C. I.; Gould, I. R.; Merz, K. M., Jr.; Ferguson, D. M.; Spellmeyer, D. C.; Fox, T.; Caldwell, J. C.; Kollman, P. A. *J. Am. Chem. Soc.* **1995**, *117*, 5179.
(23) Ángyán, J. G.; Chipot, C. *Int. J. Quantum Chem.* **1994**, *52*, 17.
(24) Chipot, C.; Ángyán, J. G. *GRID Version 3.0: Point multipoles derived from molecular electrostatic properties*; QCPE No. 655, 1994.
(25) Onsager, L. *J. Am. Chem. Soc.* **1936**, *58*, 1486.
(26) Rivail, J. L.; Rinaldi, D. *Chem. Phys.* **1976**, *18*, 233.
(27) Rinaldi, D. *Comput. Chem.* **1982**, *6*, 155.
(28) Rinaldi, D.; Pappalardo, R. R. *SCRFPAC: A self-consistent reaction field package*; QCPE No. 622, 1992.
(29) Torrie, G. M.; Valleau, J. P. *J. Comput. Phys.* **1977**, *23*, 187.
(30) Valleau, J. P.; Card, D. N. *J. Chem. Phys.* **1972**, *57*, 5457.
(31) Kumar, S.; Bouzida, D.; Swendsen, R. H.; Kollman, P. A.; Rosenberg, J. M. *J. Comput. Chem.* **1992**, *13*, 1011.
(32) Boczko, E. M.; Brooks, C. L., III. *J. Phys. Chem.* **1993**, *97*, 4509.
(33) Frisch, M. J.; Trucks, G. W.; Schlegel, H. B.; Gill, P. M. W.; Johnson, B. G.; Robb, M. A.; Cheeseman, J. R.; Keith, T.; Petersson, G. A.; Montgomery, J. A.; Raghavachari, K.; Al-Laham, M. A.; Zakrzewski, V. G.; Ortiz, J. V.; Foresman, J. B.; Peng, C. Y.; Ayala, P. Y.; Chen, W.; Wong, M. W.; Andres, J. L.; Replogle, E. S.; Gomperts, R.; Martin, R. L.; Fox, D. J.; Binkley, J. S.; Defrees, D. J.; Baker, J.; Stewart, J. P.; Head-Gordon, M.; Gonzalez, C.; Pople, J. A. *GAUSSIAN 94*; Gaussian Inc.: Pittsburgh, PA, 1995.
(34) Boys, S. J.; Bernardi, F. *Mol. Phys.* **1970**, *19*, 553.
(35) Pohorille, A.; Benjamin, I. *J. Chem. Phys.* **1991**, *94*, 5599.
(36) Linse, P. *J. Am. Chem. Soc.* **1990**, *112*, 1744.
(37) Frenkel, D.; Smit, B. *Understanding molecular simulations: From algorithms to applications*; Academic Press: San Diego, 1996.
(38) Hobza, P.; Selzle, H. L.; Schlag, E. W. *Chem. Rev.* **1994**, *94*, 1767.
(39) Chipot, C.; Jaffe, R.; Maigret, B.; Pearlman, D. A.; Kollman, P. A. *J. Am. Chem. Soc.* **1996**, *118*, 11217.
(40) Jaffe, R. L.; Smith, G. D. *J. Chem. Phys.* **1996**, *105*, 2780.
(41) McQuarrie, D. A. *Statistical mechanics*; Harper and Row: New York, 1976.
(42) Beveridge, D. L.; DiCapua, F. M. *Annu. Rev. Biophys. Biophys.* **1989**, *18*, 431.
(43) Pearlman, D. A.; Kollman, P. A. *J. Chem. Phys.* **1991**, *94*, 4532.
(44) Boresch, S.; Karplus, M. *J. Comput. Chem.* **1996**, *105*, 5145.
(45) den Otter, W. K.; Briels, W. J. *J. Chem. Phys.* **1998**, *109*, 4139.